TU Delft

Delft University of Technology

Performance assessment of a multi-fuel hybrid engine for future aircraft

Yin, Feijia; Gangoli Rao, Arvind; Bhat, Abhishek; Chen, Min

DOI
10.1016/j.ast.2018.03.005

Publication date
2018

Document Version
Final published version

Published in
Aerospace Science and Technology

Citation (APA)
Yin, F., Gangoli Rao, A., Bhat, A., & Chen, M. (2018). Performance assessment of a multi-fuel hybrid engine for future aircraft. *Aerospace Science and Technology*, *77*, 217-227. https://doi.org/10.1016/j.ast.2018.03.005

Important note
To cite this publication, please use the final published version (if applicable).
Please check the document version above.

Copyright
Other than for strictly personal use, it is not permitted to download, forward or distribute the text or part of it, without the consent of the author(s) and/or copyright holder(s), unless the work is under an open content license such as Creative Commons.

Takedown policy
Please contact us and provide details if you believe this document breaches copyrights.
We will remove access to the work immediately and investigate your claim.

This work is downloaded from Delft University of Technology.
For technical reasons the number of authors shown on this cover page is limited to a maximum of 10.

Green Open Access added to TU Delft Institutional Repository

'You share, we take care!' – Taverne project

https://www.openaccess.nl/en/you-share-we-take-care

Otherwise as indicated in the copyright section: the publisher is the copyright holder of this work and the author uses the Dutch legislation to make this work public.

Aerospace Science and Technology 77 (2018) 217–227

Contents lists available at ScienceDirect

Aerospace Science and Technology

www.elsevier.com/locate/aescte

Performance assessment of a multi-fuel hybrid engine for future aircraft

Feijia Yin [a,*], Arvind Gangoli Rao [a], Abhishek Bhat [b], Min Chen [c]

[a] Faculty of Aerospace Engineering, Delft University of Technology, Kluyverweg 1, 2629HS, Delft, Netherlands
[b] Honeywell Technology Solutions, Bangalore, India
[c] School of Energy and Power Engineering, Beihang University, China

ARTICLE INFO

Article history:
Received 7 September 2017
Received in revised form 25 February 2018
Accepted 5 March 2018
Available online 7 March 2018

Keywords:
Hybrid engine
Multi-fuel
Optimization
Performance assessment
Low emissions

ABSTRACT

This paper presents the performance assessment of a novel turbofan engine using two energy sources: Liquid Natural Gas (LNG) and kerosene, called Multi-Fuel Hybrid Engine (MFHE). The MFHE is a new engine concept consisting of several novel features, such as a contra-rotating fan to sustain distortion caused by boundary layer ingestion, a sequential dual-combustion system to facilitate "Energy Mix" in aviation and a Cryogenic Bleed Air Cooling System (CBACS) to cool the turbine cooling air. The MFHE has been envisaged as a propulsion system for a long-range Multi-Fuel Blended Wing Body (MFBWB) aircraft. In this research, we study the uninstalled characteristics of the MFHE covering three aspects: 1) the effects of CBACS on the High Pressure Turbine (HPT) cooling air requirement and its consequence on the engine cycle efficiency; 2) the cycle optimization of the MFHE; 3) the performance of the MFHE at a mission level. An integrated model framework consisting of an engine performance model, a sophisticated turbine-cooling model, and a CBACS model is used. The parametric analysis shows that using CBACS can reduce the bleed air temperature significantly (up to 400 K), thereby decreasing the HPT cooling air by more than 40%. Simultaneously, the LNG temperature increases by more than 200 K. The hybrid engine alone reduces the CO_2 emission by about 27% and the energy consumption by 12% compared to the current state-of-the-art turbofan engine. Furthermore, the mission analysis indicates a reduction in NOx emission by 80% and CO_2 emission by 50% when compared to the baseline aircraft B-777 200ER.

© 2018 Elsevier Masson SAS. All rights reserved.

1. Introduction

Aviation contributes to 5% of the total anthropogenic climate change including both the CO_2 effects and the non-CO_2 effects from NO_x emissions, water vapor and contrails [1]. The demand for air transportation is anticipated to grow by 4.6% annually for the next 20 years [2], which aggravates the aviation's climate impact. To enable the sustainable growth, the Advisory Council for Aeronautics Research in Europe has set ambitious objectives to reduce CO_2 emission by 75% and NO_x emissions by 90% by the year 2050 when compared to the year 2000 technology [3].

The CO_2 reduction can be achieved in a combination with innovative aircraft/engine technologies and using alternative fuels. The Geared Turbofan [4], the Intercooled Recuperated Aero-engine [5], and the Open rotor [6] are examples of the efficient engine concepts. Whereas, the NO_x emissions can be reduced by the innovative low NO_x combustion techniques and by using hydrogen-rich alternative fuels.

One of the other main challenges for future aviation is the energy source. Currently, aviation consumes around 1 Billion liters of Jet Fuel every day [7,8] and it is anticipated to increase with the increase in air traffic despite the improvement in aircraft efficiency. On the other hand, the oil reserves are depleting, thus creating a discrepancy in the supply and demand, which will lead to a significant increase in the fuel cost. This increase in fuel cost has already increased the fuel share in the total operating cost of an airline to around 30% [9]. Further increase in fuel prices would have negative consequences for airlines. Therefore, other means of energy source to drive the aircraft engines will have to be tapped. Though the usage of sustainable alternative fuels in the aviation industry is not widely practiced, some commercial flights have been successfully operated with biofuels [10,11]. Furthermore, the emissions standard set by the International Civil Aviation Organization for engine certification is becoming stringent. As long as the conventional fuel is in use, the goal of reducing CO_2 emission significantly remains illusive; hence, alternative fuels will play an important role.

* Corresponding author.
E-mail addresses: F.yin@tudelft.nl (F. Yin), A.gangolirao@tudelft.nl (A. Gangoli Rao), abhishek.rkbhat@gmail.com (A. Bhat), chenmin@buaa.edu.cn (M. Chen).

https://doi.org/10.1016/j.ast.2018.03.005
1270-9638/© 2018 Elsevier Masson SAS. All rights reserved.

Nomenclature

Abbreviations

BPR	Bypass Ratio
CBACS	Cryogenic Bleed Air Cooling System
CHEX	Cryogenic Heat Exchanger
EF	Energy Fraction
EI	Emission Index ..... g/kg kg/kg
FPR	Fan Pressure Ratio
HPC	High Pressure Compressor
HPT	High Pressure Turbine
ITB	Inter-stage Turbine Burner
LNG	Liquefied Natural Gas
LH2	Liquefied Hydrogen
LHV	Lower Heating Value..... J/kg
LPC	Low Pressure Compressor
LPT	Low Pressure Turbine
MFBWB	Multi-Fuel Blended Wing Body
MFHE	Multi-Fuel Hybrid Engine
OPR	Overall Pressure Ratio
SED	Specific Energy Density
SLS	Sea Level Static
TOC	Top of Climb
VED	Volumetric Energy Density
VHBR	Very High Bypass Ratio

Symbols

$\dot{m}$	Mass flow rate..... kg/s
p_t	Stagnation pressure ..... Bar
T_t	Stagnation temperature ..... K
η	Efficiency
π	Pressure ratio
ε	Heat exchanger effectiveness

Subscripts

3	High pressure compressor exit
4	High pressure turbine inlet
46	Low pressure turbine inlet

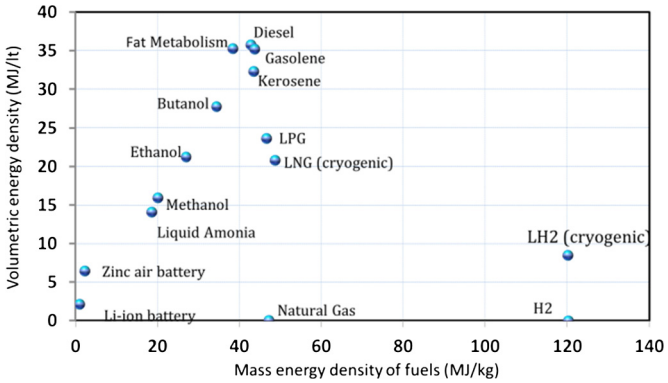

Fig. 1. Comparison of various energy sources for aviation [12].

2. Fuel selection

There are several criteria in selecting a fuel for aviation. One of the main criteria is the energy density, as reducing weight and volume is of paramount importance for aviation. Both Specific Energy Density (SED, amount of energy per unit mass of the fuel) and Volumetric Energy Density (VED, the amount of energy per unit volume) are essential. In Fig. 1, various energy sources regarding their SED and VED are presented [12]. It can be seen that Jet-A/kerosene has good SED and VED and therefore suitable for aviation. Moreover, Liquefied Hydrogen (LH2) has high SED but poor VED, implying that huge volume would be required to carry any reasonable amount of LH2. This makes it challenging to use LH2 in aviation. Additionally, using LH2 in aviation has other challenges like safety, logistics, etc. [13]. Certainly, the advantages of using LH2 should not be neglected as the CO_2 emission can be eliminated. Moreover, hydrogen should not be viewed as fuel but as an energy carrier (e.g., high-energy dense battery). From a long-term perspective, LH2 can be a good candidate for aviation, especially, to satisfy the imperative requirement for sustainability.

Furthermore, the Liquefied Natural Gas (LNG), which primarily consists of methane, has drawn considerable attention. LNG is natural gas that has been liquefied form to increase energy density and avoid pressurization. From Fig. 1, it can be seen that LNG lies in between kerosene and LH2, both in terms of SED and VED. Currently, LNG is one of the cheapest fuels available [14]. The global reserves of natural gas are enormous, thus implying that the LNG price would be stable. Moreover, LNG is one of the cleanest fuels, and recently it has been shown that LNG can also be generated by using renewable energy [15,16]. The effects of using LNG for civil aviation are summarized below.

Advantages of LNG:

- Approximately 25% reduction in CO_2 emission for the same energy consumption
- The natural gas can be mixed with air in a better way than kerosene, which reduces NOx emission.
- LNG is a cryogenic fuel and therefore a good heat sink. It can be used beneficially to enhance the thermodynamic efficiency of the engine, for instance by intercooling, bleed cooling, air-conditioning, etc.
- LNG is cheaper than the conventional jet fuel in terms of MJ/$.
- The energy density of LNG is higher than kerosene

Disadvantages of LNG:

- Unlike kerosene, LNG cannot be stored in wings.
- LNG has to be stored in insulated cylindrical or spherical tanks, increasing the aircraft operating empty weight.
- The volumetric energy density of LNG is lower compared to kerosene.
- Airport facilities and logistics for storing and tanking LNG are required.
- The H_2O emission (an import greenhouse gas at higher altitudes and latitudes) of burning LNG is higher compared to kerosene.

3. The multi-fuel blended wing body aircraft

Cryogenic fuels, like LNG, need to be stored in insulated cylindrical or spherical tanks with the well-insulated system to prevent them from leaking and boiling off. Therefore, the volume required to carry cryogenic fuels increases significantly, which makes it challenging for conventional aircraft. The Blended Wing Body (BWB) concept provides possibilities for cryogenic fuels as far as space is concerned. The BWB has been studied by many researchers world widely [17–20]. The MFBWB concept proposed in

Fig. 2. Schematic of the MFBWB concept.

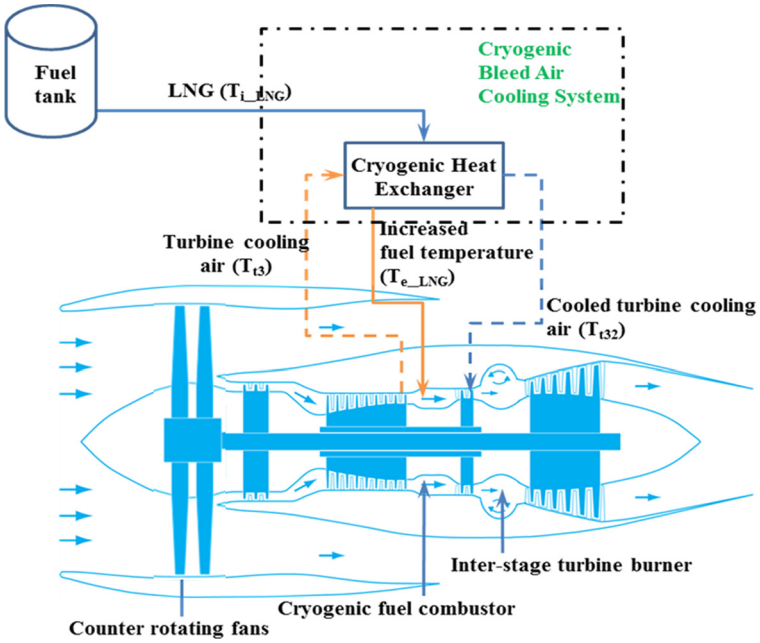

Fig. 3. The schematic of the hybrid engine concept using LNG & kerosene.

the AHEAD project[1] is one of these radical concepts. A schematic of the MFBWB aircraft is depicted in Fig. 2. In this specific configuration, the LNG fuel tanks are placed at the rear of the aircraft. The features of the MFBWB are listed as below [21]:

- 300 passengers capacity
- Design range of 14000 km
- Carrying multiple fuels, such as LNG and kerosene/biofuel
- Utilizing Boundary Layer Ingestion (BLI) technology
- Low NO_x and CO_2 emissions

4. The multi-fuel hybrid engine

To exploit the unique opportunities provided by the MFBWB aircraft, a novel Multi-fuel Hybrid Engine (MFHE) concept has been proposed (see Fig. 3). The MFHE is conceived based on an Inter-stage Turbine Burner (ITB) turbofan engine for the following reasons. Firstly, the dual combustion chamber configuration enables different fuels to be used simultaneously (LNG and kerosene in this paper). This way, the space usage within an airframe can be optimized with respect to energy storage while restricting the increase in fuel volume and the associated aerodynamic drag. Secondly, the LNG is used in the first combustor (the main burner), while the kerosene is used in the ITB. By changing the energy split ratio between the LNG and kerosene, the reduction in engine emissions can be optimized. Moreover, as the Very High Bypass Ratio (VHBR) and Overall Pressure Ratio (OPR) become imperative for a turbofan engine to improve its efficiency, meeting the off-design performance (e.g. the flat rated temperature) is challenging. The study in [22] shows that using an ITB in a VHBR turbofan can help to improve the engine off-design performance.

The distinguished features of the MFHE are summarized as below:

- Contra-Rotating Fans (CRF): The MFBWB intends to ingest the boundary layer flow over the airframe to improve the propulsion efficiency. To better sustain the non-uniform inlet flow caused by the Boundary Layer Ingestion (BLI) [23], the normal fan is replaced by the CRF in the hybrid engine.
- The hybrid combustion system: The reduction in NO_x emission of the hybrid engine is approached by two means. The first being the advanced low NO_x combustion techniques (premixed combustion in the first combustion chamber and flameless combustion in ITB) are used. The second approach is that the engine with sequential combustor has lower maximum operating temperature compared to the single combustor engine for the same power output, thereby lowering the NO_x emission further. The thorough analysis has been performed to study the emissions of the hybrid combustion system, where the results confirm a substantial reduction in NO_x emission in the hybrid engine [24].

[1] http://www.ahead-euproject.eu/.

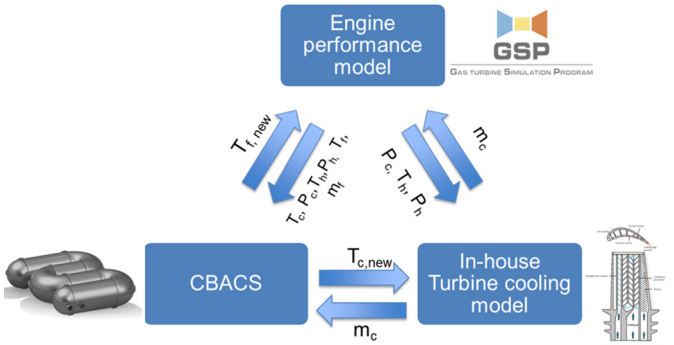

Fig. 4. The interactions between three sub models.

- The Cryogenic Bleed Air Cooling System (CBACS): The Cryogenic Bleed Air Cooling System in the hybrid engine is another non-conventional feature (see the upper part of Fig. 3). In the modern aircraft engines, a large amount of air (about 30% of the core air mass flow) is bled off the compressor to cool the turbine blade. Using such significant amount of cooling penalizes the turbine efficiency by more than 10% [25]. Moreover, the engine core size has become much smaller as the geared turbofan engine configuration is used. The engine off-design performance, e.g., the compressor surge margin is more sensitive to the air bleed. Therefore, the urgency of reducing the turbine cooling air is strong. The CBACS in the hybrid engine is expected to fulfill such an imperative.

The core element of the CBACS is a cryogenic heat exchanger (CHEX). In the heat exchanger, the cryogenic fuel (LNG) serves as a coolant to pre-cool the HPT cooling air, thereby reducing the HPT cooling requirement. Moreover, the fuel temperature is increased at the exit of the heat exchanger, hence will save fuel consumption. Overall, the engine cycle would become more efficient. The details about the hybrid engine philosophy can be found in [12].

5. The multi-fuel hybrid engine model

In order to evaluate the MFHE performance, a modeling framework is created which consists of an engine performance model, a sophisticated in-house turbine-cooling model and a cryogenic bleed air cooling system (CBACS) model. The interactions between these three sub-models are described in Fig. 4. The notations in this figure can be found in Table 1.

5.1. The engine performance model

The configuration of the hybrid engine is unconventional; therefore, a flexible modeling environmental is required to model such an engine concept. In the current analysis, the Gas turbine Simulation Program (GSP) is used to model the hybrid engine [26].

Table 1
The descriptions of the variables in Fig. 4.

Notations	Descriptions	Units
T_c	Initial cooling air temperature	K
$T_{c,\,new}$	Reduced cooling air temperature via CBACS	K
P_c	Cooling air pressure	Pa
m_c	Cooling air mass flow	kg
T_f	Fuel temperature (LNG)	K
$T_{f,\,new}$	Increased fuel temperature via CBACS	K
m_f	Fuel mass flow	kg
T_h	Hot gas temperature	K
P_h	Hot gas pressure	Pa

The model layout is shown in Fig. 5. The main gas path consists of inlet, fan, Low Pressure Compressor (LPC), High Pressure Compressor (HPC), main combustion chamber (burning natural gas), High Pressure Turbine (HPT), Inter-stage Turbine Burner (ITB, burning kerosene/biofuels), Low Pressure Turbine (LPT), core nozzle and bypass nozzle. An adiabatic duct (component number 23 in Fig. 5) is applied to consider the bypass pressure loss. The hybrid engine uses a Contra-rotating Fans (CRF), which is driven by a geared system. The losses caused by such a geared system are considered as a fraction of the total losses through the LPT, represented by the LPT mechanical efficiency. Furthermore, in the bleed control components (numbered as 2–6 and 9), the turbine cooling is specified as a fraction of the core air mass flow rate, which is extracted from specific HPC stages depending on the pressure of the hot gas. The component numbered 8 is a generic scheduler to set up the engine thrust requirement at given operating conditions [27].

The fundamental equations, which GSP follows to calculate the component characteristics and the overall engine performance, can be found from standard textbooks on gas turbine theory [28,29]. The modeling procedure follows the convention of starting with a reference point (also named as the engine design condition) followed by the off-design performance calculations. The component efficiencies and the pressure losses at the design condition (cruise) of the hybrid engine are given in Table 2. For the off-design performance calculation, the generic compressor and turbine maps are scaled according to the design condition. For the contra-rotating fans, a different map was created using the data taken from the available public literature [30], and then scaled based on the design performance of the CRF in the current study. The map for the CRF is shown in Fig. 6.

The performance requirements of the hybrid engine at different operating points are given in Table 3. These values are derived from the design of MFBWB aircraft over different flight segments in the aircraft mission analysis.

5.2. The turbine cooling prediction model

The technological development trend is driving up the OPR and TIT of the modern gas turbines. Consequently, the effect of the bleed air cooling on the engine performance is becoming increas-

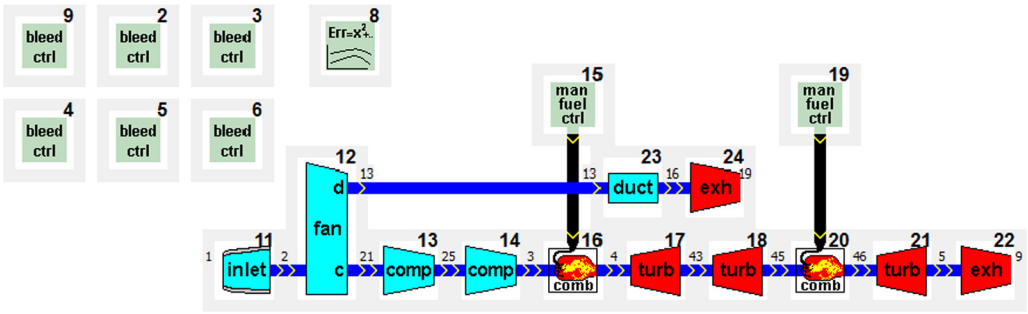

Fig. 5. The engine performance model.

Table 2
Baseline component performance parameters.

Component	Performance parameter	Notation	Datum value	Unit
Fan	polytropic efficiency	η_{fan}	93	%
LPC	polytropic efficiency	η_{LPC}	93	%
HPC	polytropic efficiency	η_{HPC}	91	%
Main combustor	combustion efficiency	η_{CC}	99.9	%
	pressure ratio	π_{CC}	0.95	[–]
HPT (uncooled)	polytropic efficiency	η_{HPT}	93	%
ITB	combustion efficiency	η_{ITB}	99.7	%
	pressure ratio	π_{ITB}	0.97	[–]
LPT (uncooled)	polytropic efficiency	η_{LPT}	92.5	%
HP shaft	mechanic efficiency	η_{mHP}	99.5	%
LP shaft	mechanic efficiency	η_{mLP}	99.3	%
Bypass duct	pressure loss	$\Delta p_t/p_{tin}$	2	%

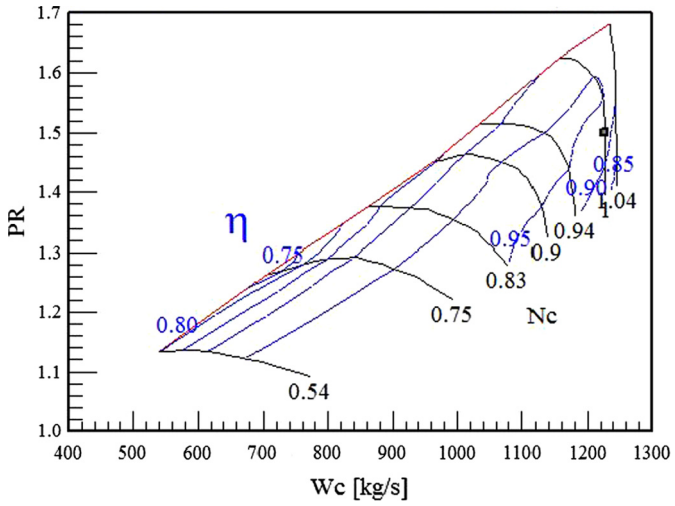

Fig. 6. Scaled contra-rotating fan map.

Table 3
The performance requirements from hybrid engine.

Operating points	Ambient condition	Mach number	Thrust [kN]
Max static	Sea Level Static (SLS) ISA	0	280
Hot day takeoff	SLS, ISA+15 K	0	280
Take-off	SLS ISA	0.2	250
Top of climb (TOC)	12 km, ISA	0.8	56
Cruise	12 km, ISA	0.8	50
Ground idle	SLS ISA	0	20

ingly important. During the cycle analysis phase, the cooling bleed air is often modeled by simplified correlations, which can fail to capture the nonlinear features hence having a risk of overestimating the engine performance.

In the current analysis, the effects of the bleed cooling system play significant roles to assess the engine performance. Therefore, a physics-based in-house turbine cooling prediction tool using semi-empirical correlations for heat transfer and pressure losses has been used. Details of the developed models have been elaborated in [31,32].

The turbine cooling model reads in the temperature and pressure of the coolant, the temperature and pressure of the hot gas, as well as the maximum allowable metal temperature. By following the procedure in Fig. 7, the amount of cooling air required and the resulting pressure losses can be calculated. As one can notice, the turbine-cooling model requires information on the geometry of a turbine vane or blade. In the current model, a typical turbine blade configuration used in the modern aero engines, as demonstrated in Fig. 8, is applied. The maximum allowable metal temperature is 1450 K.

5.3. The Cryogenic Bleed Air Cooling System (CBACS) model

The integration of the CBACS and the engine main gas path is demonstrated in Fig. 9, where, the HPT cooling bleed air is pre-

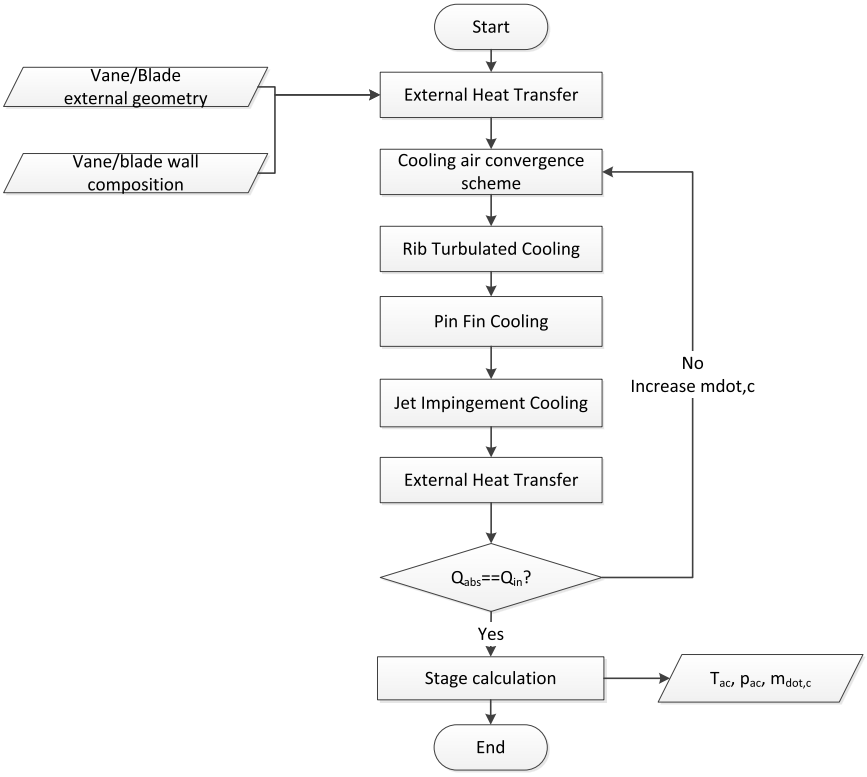

Fig. 7. The overview of the turbine cooling model working principle [32].

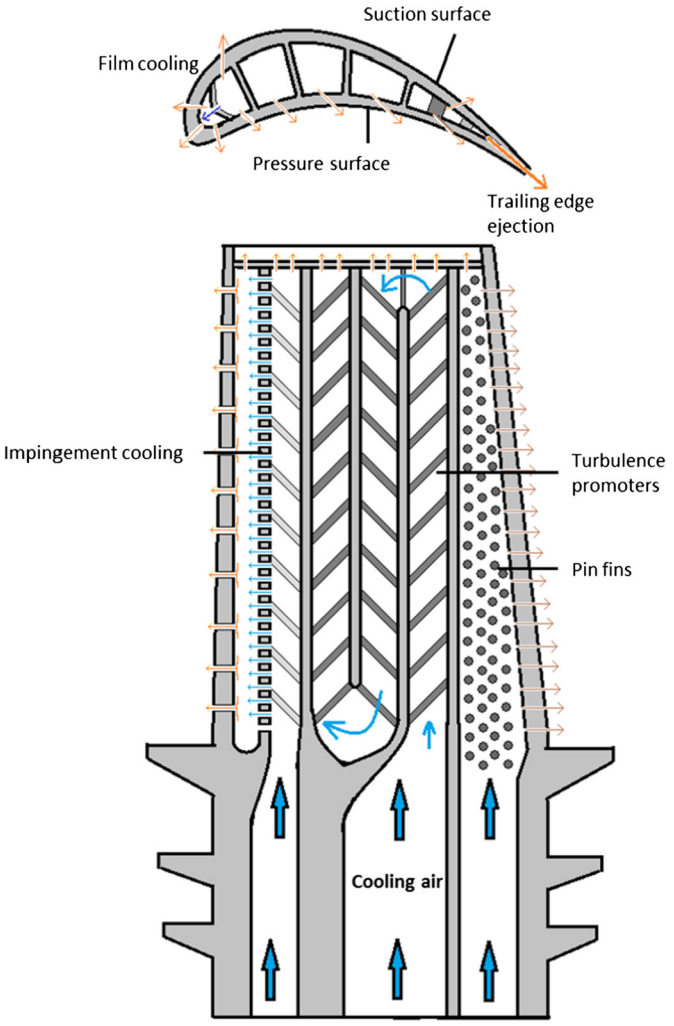

Fig. 8. Schematic of an advanced aero engine cooled high-pressure turbine blade.

cooled by LNG via a cryogenic heat exchanger (CHEX). One of the noticeable phenomena observed in the CHEX is the phase change of LNG. When the temperature of LNG reaches its boiling point (120 K at 1 Bar atmospheric pressure), LNG starts to vaporize. This phase change is beneficial in increasing the heat transfer coefficient. However, it has a negative effect on the pressure drop due to the acceleration of the flow.

Table 4
Specifications of heat exchanger design.

Design variables	Values
Inlet bleed air temperature, K	T_{t3}
Exit bleed air temperature, K	600
Inlet fuel temperature, K	120
Inlet bleed air pressure, Bar	p_{t3}
Air/fuel mass flow rate, kg/s	Determined by cycle calculation
Bleed air pressure loss ($\Delta p/p_{t3}$), %	≤3

Table 5
Heat exchanger geometrical specifications.

Description	Parameter
Length (straight pipe) [m]	2.46
Outer shell diameter [m]	0.26
Inner tube diameter [m]	0.026
Wall thickness tube [m]	0.001
Number of units [–]	3

The air–LNG CHEX for the MFHE has been carefully designed by Fohmann [33]. The design condition is at cruise. A shell-tube configuration with fins in a counter-flow arrangement is considered following a typical two-phase flow heat exchanging mechanism. The heat exchanger design parameters are specified in Table 4. They are pressure, temperature, and mass flow rate of both fluids at the inlet. The temperature of the bleed air at the exit is another design variable to determine the total heat to be transferred. These parameters have been taken based on the parametric analysis conducted above. The cycle performance calculation determines the mass flow rate of LNG and cooling air. It should be noted that the pressure drop of the bleed air should be significantly lower than the combustor pressure drop to enable successful mixing of the film cooling air with the mainstream flow through the turbine. In Fig. 10, the layout of the heat exchanger design (Fig. 10(B)) and the cross-section (Fig. 10(A)) are depicted, with the main geometrical specifications given in Table 5.

After the dimension of the heat exchanger is calculated, the performance of the heat exchanger at other operating conditions is determined. The characteristics of the heat exchanger are represented by its effectiveness. The definition of the heat exchanger effectiveness follows the ε-NTU method presented by Shah and

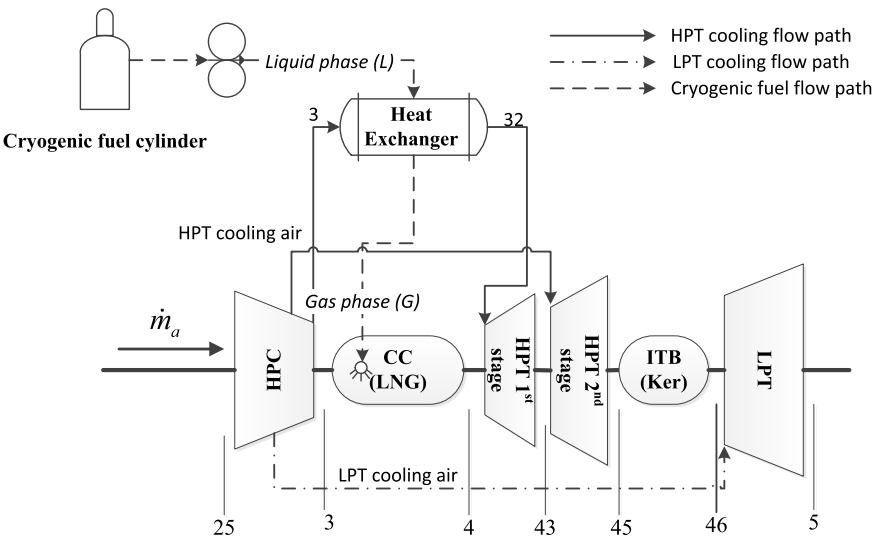

Fig. 9. Overview of the turbine cooling flow path.

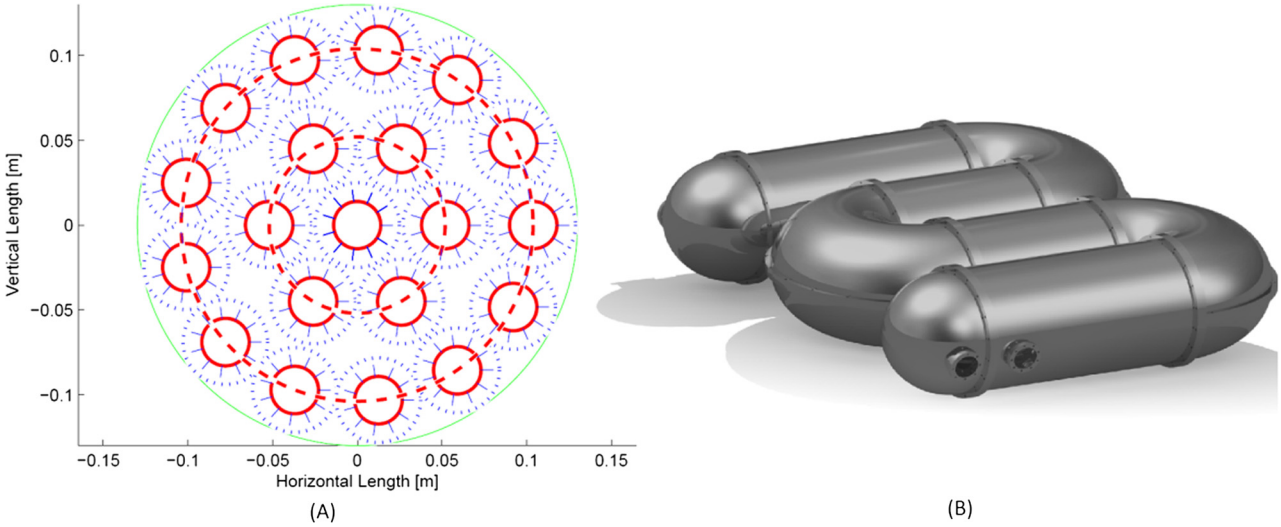

Fig. 10. Schematic of the heat exchanger: (A) Cross section of the heat exchanger, (B) the complete layout [33].

Sekulic in [34]. The maximum temperature difference together with the mass flow rate and the heat capacity of fluids determine the maximum heat flux, represented by Eqn. (1),

$$q_{\max} = \min\left\{\dot{m}_{air}\cdot\left(h(T_{t3}) - h(T_{i\_LNG})\right), \dot{m}_{LNG} \cdot \left(h(T_{t3}) - h(T_{i\_LNG})\right)\right\} \tag{1}$$

where min indicates the minimum heat flux between two fluids; h represents the specific enthalpy of given substance; $\dot{m}$ is the mass flow rate of given fluid; the subscript 3 indicates the inlet condition of the air, and *i_LNG* indicates the inlet condition of LNG. After defining the maximum heat flux, the effectiveness of the CHEX can be calculated by Eqn. (2),

$$\varepsilon = \frac{q}{q_{\max}} = \frac{\dot{m}_{LNG}\cdot\left(h(T_{e\_LNG}) - h(T_{i\_LNG})\right)}{q_{\max}} = \frac{\dot{m}_{air}\cdot\left(h(T_{t3}) - h(T_{t32})\right)}{q_{\max}} \tag{2}$$

where the subscripts 3 and 32 indicate the inlet and exit of the bleed air section (in line with Fig. 3); *e_LNG* and *i_LNG* indicate the LNG at exit and inlet respectively.

In order to incorporate the CHEX performance characteristics into the engine performance model, a CHEX performance map was generated as shown in Fig. 11. The map describes the variation in heat exchanger effectiveness as a function of mass flow rates in air and LNG. The design effectiveness of the heat exchanger is 50%. This performance map is implemented in the hybrid engine performance model. It can be seen that the effectiveness decreases for off-design conditions.

6. Engine performance evaluation

Using the models described in the previous section, the performance of the hybrid engine is investigated.

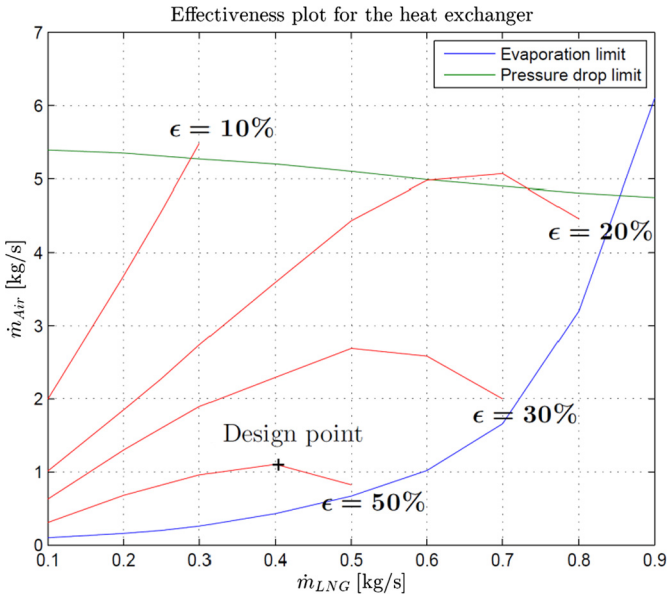

Fig. 11. The variation of the effectiveness of the heat exchanger versus the fluid mass flow rate.

6.1. The engine performance optimization at cruise

The cycle optimization is performed to minimize the specific fuel consumption at cruise. The design space and constraints are defined in Table 6. The optimization has been conducted with respect to the ITB energy fraction (defined by Eqn. (3), where "ker" denotes kerosene) from 0 to 0.3. The inlet mass flow rate is kept constant in order to compare engines with the same diameter (and thus similar installation penalties). The optimization results of

Table 6
Definition of engine design space and constraints.

Design space formed by design parameters		Optimization constraints	
Fan Pressure Ratio (FPR)	[1.2, 1.5]	Overall Pressure Ratio (OPR)	≤70
LPC pressure ratio	[1.4, 5.0]	FN [kN]	= 50
HPC pressure ratio	[8, 20]	Inlet mass flow rate [kg/s]	constant
HPT inlet temperature (T_{t4}) [K]	[1400, 1900]	ITB energy fraction	0, 0.1, 0.2, 0.3
Bypass Ratio (BPR)	[8, 15]		

Table 7
The optimized hybrid engine cycle including CBACS at cruise condition.

	ITB energy fraction			
	0	0.1	0.2	0.3
Design parameters				
BPR	15	15	15	15
FPR	1.48	1.48	1.48	1.48
LPC pressure ratio	5	5	5	5
HPC pressure ratio	9.48	9.48	9.48	9.48
HPT inlet temperature [K]	1593	1521	1451	1387
LPT inlet temperature [K]	1177	1187	1200	1215
Engine performance				
Thermal efficiency [%]	52.5	51.7	50.7	49.7
Propulsive efficiency [%]	82.6	82.6	82.6	82.6
LNG mass flow rate [kg/s]	0.54	0.50	0.45	0.40
Kerosene mass flow rate [kg/s]	0	0.06	0.13	0.20
Bleed air temperature [K]	602	603	604	604
LNG temperature [K]	528	478	424	366

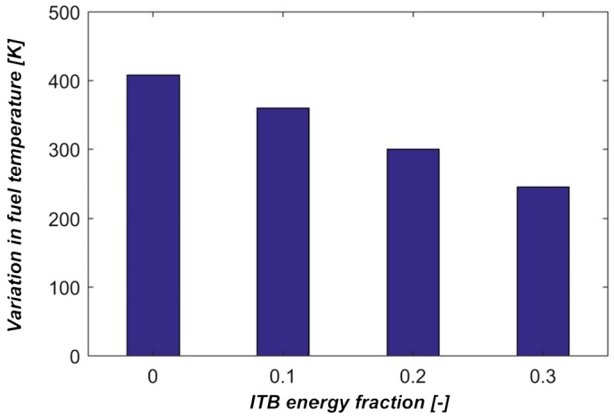

Fig. 12. Variation in fuel temperature (LNG) at the exit of the exchanger versus ITB energy fraction with respect to the non-CBACS ITB turbofan engine at the same ITB energy fraction.

the multi-fuel hybrid engine are presented in the following paragraphs.

$$ITB\,EF = \frac{\dot{m}_{bio} \times LHV_{\text{ker}}}{\dot{m}_{LNG} \times LHV_{LNG} + \dot{m}_{\text{ker}} \times LHV_{\text{ker}}} \tag{3}$$

The optimal performance of the hybrid engine at different ITB energy fractions is presented in Table 7. As the ITB energy fraction increases, the HPT inlet temperature reduces from 1593 K to 1387 K. The LPT inlet temperature of each engine cycle remains nearly constant at around 1200 K. The bleed air temperature is about 600 K and is nearly constant regardless of the ITB energy fraction (as this is the design requirement for the heat exchanger). The engine thermal efficiency decreases as the ITB energy fraction increases, as more heat is added at lower pressure in the cycle. The mass flow rate of kerosene increases with increase in the ITB energy fraction whereas the mass flow rate of LNG decreases.

In order to assess the impact of CBACS on the design performance of the hybrid engine, the engine performance in Table 7 is compared to the engines with multi-fuel configurations but excluding the CBACS system. The variation in fuel temperature and the resulting turbine cooling requirement is presented in Fig. 12 and Fig. 13 respectively. Compared to the original LNG temperature (120 K), the fuel temperature at the exit of the heat exchanger increases by 200 K at the ITB energy fraction of 0.3 and up to 400 K at the ITB energy fraction of 0 (Fig. 12). Also, the turbine cooling air requirement can be reduced by around 45%, as can be observed in Fig. 13 because of the lower bleed air temperature via CBACS.

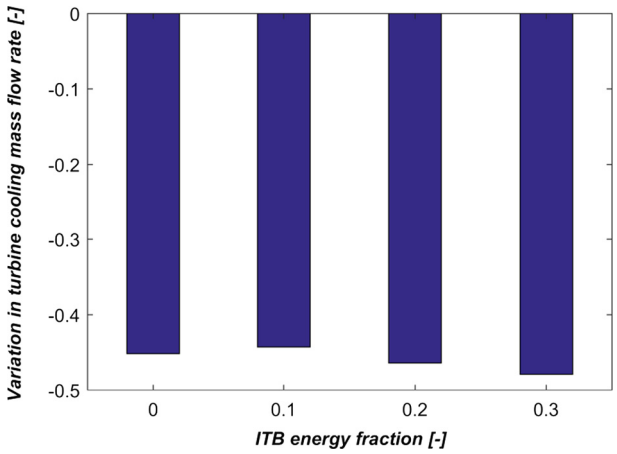

Fig. 13. Variation in turbine cooling mass flow rate versus ITB energy fraction. The negative sign indicates the reduction of cooling mass flow rate with respect to the non-CBACS ITB turbofan engine at the same ITB energy fraction.

Table 8
The operating limits of the hybrid engine.

Variables	Notation	Value	Description
High pressure spool speed [%]	N2	100	Max
Low pressure spool speed [%]	N1	100	Max
Fan surge margin [%]	SM_fan	10	Min
LPC surge margin [%]	SM_LPC	20	Min
HPC surge margin [%]	SM_HPC	25	Min
HPC exit temperature [K]	T_{t3}	1000	Max
HPT inlet temperature [K]	T_{t4}	1800	Max
LPT inlet temperature [K]	T_{t46}	1450	Max

Table 9
Engine characteristics at sea level static conditions.

	ITB energy fraction			
	0	0.1	0.2	0.3
FN [kN]	280	280	280	280
Flat rated temperature	ISA-30 K	ISA-3 K	ISA+13 K	ISA+18 k

6.2. The verification of the optimized engine cycle

This section is focused on the verification of the optimized engine cycle concerning the ITB energy fractions from 0 to 0.3. The analysis is performed to examine if each of the engine cycles would meet the performance requirements at off-design conditions elaborated in Table 3. The operating limits in Table 8 are considered. The LPT inlet temperature (T_{t46}) is limited below 1450 K such that no LPT cooling would be required.

The engine characteristics at the sea level static conditions can be found in Table 9. We can notice that even though the design performance of the single combustor engine is the best, the engine fails to deliver the thrust required at sea level static conditions. As the energy addition in the ITB increases, the engine core becomes more powerful. The optimized engine can meet the constraints while delivering the thrust. The same procedure has been performed to examine if each engine can meet the requirement in Table 3. Eventually, the engine designed with the ITB energy fraction of 0.3 was selected and will be used for the mission analysis in the next section.

6.3. Evaluation of the hybrid engine performance at cruise level

To evaluate the performance of the optimized hybrid engine cycle, three baseline engines listed below are used. The performance of these engines at cruise condition is displayed in Table 10. The

Table 10
The baseline engine performance at cruise condition.

	GE90-94B[a]	GEnx-1B64	GTF-2035
Design parameters			
BPR	8.1	9.1	15
FPR	1.65	1.65	1.44
OPR	40	41	70
Tt4 [K]	1380	1438	1900
Engine performance			
Thrust [kN]	69	54	50
TSFC [g/kN/s]	15.6	14.1	13.2
Kerosene [kg/s]	1.08	0.76	0.66

[a] The GE90-94B engine data source is: https://web.stanford.edu/~cantwell/AA283_Course_Material/GE90_Engine_Data.pdf.

performance of the GTF-2035 engine has been optimized at cruise condition for the same thrust requirement as the hybrid engine.

- GE90-94B, representing an engine from the year 2000
- GEnx-1B64, representing the current state of art (SOA) engine technology
- GTF-2035, an imaginary Very High Bypass Ratio (VHBR) turbofan engine for the year 2035

A comparison has been made between the hybrid engine with the ITB energy fraction of 0.3 in Table 7 and the three baseline engines presented in Table 10. A direct TSFC comparison is not possible due to the different energy sources used in the MFHE. Instead, the engines are compared by energy consumption as defined in Eqn. (4),

$$Energy\ consumption = \dot{m}_{fuel} \cdot LHV_{fuel} \tag{4}$$

where LHV is the Lower Heating Value of the given fuel type (42.8 MJ/kg for kerosene and 50 MJ/kg for LNG); $\dot{m}_{fuel}$ is the fuel mass flow rate. The energy consumption of the hybrid engine would be the energy summation of kerosene and LNG.

The comparisons are made for the energy consumption, the CO_2 emission, and the H_2O emission (Fig. 14). As compared to the GE90 engine, the hybrid engine scores higher in all three aspects. When compared to the GEnx engine, the hybrid engine is about 12% energy efficient and is able to reduce the CO_2 emission by about 27% due to LNG. The H_2O emission is increased by about 20%. When compared to the future engine technology (GTF-2035), the hybrid engine can reduce the CO_2 emissions by 17% at the cost of 1% higher energy consumption. The H_2O emission, in this case, is about 40% higher.

6.4. Performance at mission level

This section focuses on the performance of the hybrid engine with MFBWB aircraft for a given mission. Even though the engine cycle optimization was conducted for different ITB energy fractions, after iteration with the MFBWB design process, the hybrid engine with an ITB energy fraction of 0.3 was selected. Therefore, the mission analysis has been mainly conducted for an ITB energy fraction of 0.3. A simplified mission profile, consisting of flight conditions at take-off, top of climb and cruise, is used. Three city pairs,

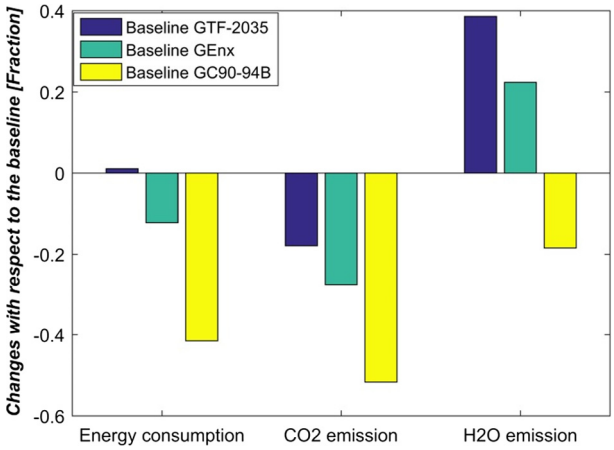

Fig. 14. The variation in the energy consumption of the hybrid LNG–kerosene hybrid engine to three baseline engines: GE90-94B, GEnx-1B64, and artificial GTF-2035.

representing different flight distances, are presented. For comparison, long-range Boeing 787-8 and Boeing 777-200ER are selected as baseline aircraft, representing the year 2000 and 2015 technology respectively.

To calculate emissions of the hybrid engine, the emission index presented in Table 11 are used. The emission index of CO_2 and H_2O are calculated assuming a complete combustion process for LNG and kerosene. The NO_x emission index has been calculated using a detailed chemical reaction network model [24], which was developed in the AHEAD project for emission predictions of the hybrid engine.

The Piano X [35], an aircraft performance analysis tool, is used to generate mission profiles for B787 and B777. With this calculation tool, emissions of an existing aircraft for a given flight mission can be predicted with fairly good accuracy. Assuming the same amount of payload and the same flight distance as used in Piano X for Boeing 777-200ER and Boeing 787-8, the emissions and energy consumption of the hybrid engine are compared with respect to per unit payload and kilometer distance. The results for various aircraft are presented in Tables 12–14. In addition to the hybrid engine, the superior aerodynamic characteristics of the MFBWB aircraft reduce the thrust requirement and therefore the fuel consumption even further.

The comparison is presented in Fig. 15 and Fig. 16. In Fig. 15, it can be observed that compared to B777-200ER, the proposed LNG–kerosene MF-BWB aircraft can reduce the NO_x emissions by more than 80%, CO_2 by 50%, and H_2O by 20%. The total energy consumption is lower by 40% for the MFBWB aircraft. When compared to the B787-8, a similar trend can be observed as depicted in Fig. 15. An exception is the H_2O emission. As the mission range decreases, the LNG–kerosene BWB might emit more H_2O than B787-8.

The reduction in CO_2 emission is beneficial for mitigating the climate impact, whereas, the effects of the increased H_2O emission on the climate is more complicated. On the one hand, the water vapor itself is a greenhouse gas; on the other hand, more H_2O might increases the possibility of contrails formation, which is an import element in the climate impact of aviation. Thorough analysis has been conducted by the AHEAD team to evaluate the overall

Table 11
Emission index used for the hybrid engine.

	Take-off		TOC		Cruise	
	1st combustor (LNG)	ITB (kerosene)	1st combustor (LNG)	ITB (kerosene)	1st combustor (LNG)	ITB (kerosene)
EI NO_x [g/kg]	8.25	14.52	3.5	8.8	2.1	7.4
EI CO_2 [kg/kg]	2.75	3.16	2.75	3.16	2.75	3.16
EI H_2O [kg/kg]	2.25	1.24	2.25	1.24	2.25	1.24

Table 12
The emissions and energy consumption per payload per unit distance (SYD-DXB 12000 km).

	B777-200ER	B787-8	LNG–kerosene BWB
Energy consumption, kJ/payload/km	8.3	7.1	4.95
NO_x emission, mg/payload/km	3.12	1.93	0.4
CO_2 emission, mg/payload/km	610.65	522.78	297.45
H_2O emission, mg/payload/km	242.32	207.45	201.58

Table 13
The emissions and energy consumption per payload per unit distance (AMS-EZE 11000 km).

	B777-200ER	B787-8	LNG–kerosene BWB
Energy consumption, kJ/payload/km	7.63	6.54	4.77
NO_x emission, mg/payload/km	2.89	1.81	0.38
CO_2 emission, mg/payload/km	561.5	481.4	286.7
H_2O emission, mg/payload/km	222.8	191	194.3

Table 14
The emissions and energy consumption per payload per unit distance (MAD-PVG 10000 km).

	B777-200ER	B787-8	LNG–kerosene BWB
Energy consumption, kJ/payload/km	6.62	5.78	4.67
NO_x emission, mg/payload/km	2.56	1.6	0.36
CO_2 emission, mg/payload/km	487.5	425.2	280.7
H_2O emission, mg/payload/km	193.4	168.7	190.2

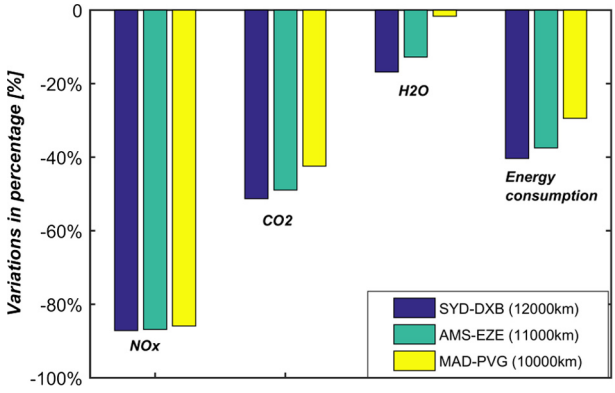

Fig. 15. Comparison of the MFBWB to B777-200ER.

climate impact of the hybrid engine. The results confirm that the multi-fuel hybrid engine together with the MFBWB reduces the climate impact by more than 20% compared to the contemporary aircraft technology level [36].

7. Conclusions and discussions

7.1. Conclusions

This paper presents the performance analysis of a novel multi-fuel hybrid engine. Both on-design and off-design performance of this novel engine concept has been investigated. Following conclusions can be drawn from the research carried out:

- The proposed engine architecture with inter-turbine burner allows the usage of two energy sources (LNG and Biofuel) simultaneously.
- By introducing a cryogenic bleed air cooling system, the bleed air temperature can be reduced by 400 K, and the LNG temperature can be increased by more than 200 K. As a result, the turbine cooling air mass flow rate can be decreased by 45%.
- Compared to the current state of the art turbofan engine, the hybrid engine reduces energy consumption by around 12% and the CO_2 emission by 27%.
- Compared to B777-200ER, the MFBWB reduces the NOx emissions by more than 80%, CO_2 emission by 50%.
- Compared to B787-8, the maximum reductions in the NOx emissions, CO_2 emission, and the energy consumption are about 80%, 40%, and 30% respectively. However, there is a slight increase in the H_2O emission.
- The hybrid engine along with MF-BWB aircraft paves a new approach of making aviation more sustainable.

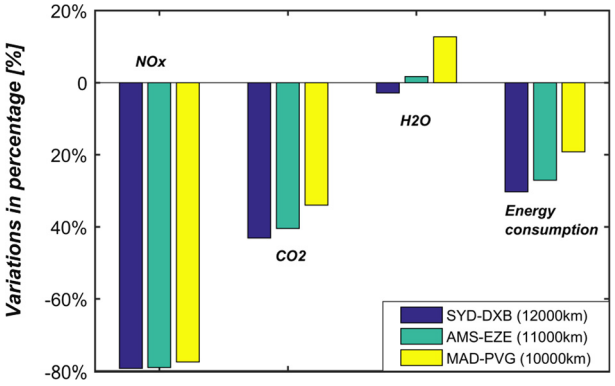

Fig. 16. Comparison of the MFBWB to B787-8.

7.2. Discussions

In this paper, we have analyzed the design and off-design performance of the multi-fuel hybrid engine in the uninstalled condition. The results prove the potential of MFHE concept in terms of the emissions reduction. The installation effects of the MFHE engine with BLI system should be investigated further as it has the potential to increase the system propulsive efficiency. However, the effect of BLI on the intake pressure ratio, flow distortion, and fan efficiency should be taken into account while evaluating the installed engine performance with BLI.

Conflict of interest statement

There is no conflict of interest.

Acknowledgements

The authors would like to acknowledge the support of all consortium members of the AHEAD project. Furthermore, the authors also would like to thank K.G. Fohmann for his contributions on the heat exchanger modeling.

Funding

Research leading to these results has received funding from the European Union Seventh Framework Programme (FP7/2007-2013) under grant agreement No. 284636.

References

[1] D.S. Lee, D.W. Fahey, P.M. Forster, P.J. Newton, R.C.N. Wit, L.L. Lim, B. Owen, R. Sausen, Aviation and global climate change in the 21st century, Atmos. Environ. 43 (22–23) (2009) 3520–3537, https://doi.org/10.1016/j.atmosenv.2009.04.024.
[2] Airbus, Growing Horizons 2017/2036, Airbus, Toulouse, France, 2017.
[3] Advisory Council for Aeronautics Research in Europe (ACARE), Flightpath 2050 Europe's Vision for Aviation, Publications Office of the European Union, Luxembourg, 2011.

[4] C. Riegler, C. Bichlmaier, The geared turbofan technology—opportunities, challenges and readiness status, in: 1st CEAS European Air and Space Conference, Berlin, Germany, 2007, pp. 10–13.
[5] S. Boggia, K. Rud, Intercooled recuperated gas turbine engine concept, in: 41st AIAA/ASME/SAE/ASEE Joint Propulsion Conference & Exhibit, Tucson, 2005.
[6] Sustainable and Green Engines (SAGE), [cited 2017 1st August], Retrieved from: http://www.cleansky.eu/sustainable-and-green-engines-sage.
[7] Aviation Outlook, International Civil Aviation Organization, 2010.
[8] Forecasting Air Traffic and Corresponding Jet-Fuel Demand Until 2025, IFP Energies Nouvelles, 2010.
[9] B. Pearce, Profitability and the air transport value chain, IATA Economics Briefing No. 10, 2013.
[10] History – KLM Corporate, [cited 2017 August 22], Retrieved from: https://www.klm.com/corporate/en/about-klm/history/.
[11] Finnair's scheduled commercial biofuel flight marks a step towards more sustainable flying, says airline, [cited 2017 August 22], Retrieved from: http://www.greenaironline.com/news.php?viewStory=1300.
[12] A.G. Rao, F. Yin, J.P. van Buijtenen, A hybrid engine concept for multi-fuel blended wing body, Aircr. Eng. Aerosp. Technol. 86 (6) (2014) 483–493, https://doi.org/10.1108/AEAT-04-2014-0054.
[13] S. Rondinelli, R. Sabatini, A. Gardi, Challenges and benefits offered by liquid hydrogen fuels in commercial aviation, in: Practical Responses to Climate Change (PRCC), 2014, Melbourne, Australia, 2014.
[14] A. Nicotra, LNG is the sustainable fuel for aviation, in: 25th World Gas Conference—Gas: Sustainable Future Global Growth, Kuala Lumpur, Malaysia, 2012.
[15] S. Kumar, S. Suresh, S. Arisutha, Production of renewable natural gas from waste biomass, J. Inst. Eng. (India), Ser. E 94 (1) (2013) 55–59, https://doi.org/10.1007/s40034-013-0021-x.
[16] Renewable Natural Gas (Biomethane) Production, 2017, [cited 2017 August 28], Retrieved from: https://www.afdc.energy.gov/fuels/natural_gas_renewable.html.
[17] R.H. Liebeck, Design of the blended wing body subsonic transport, J. Aircr. 41 (1) (2004) 10–25, https://doi.org/10.2514/1.9084.
[18] N. Qin, A. Vavalle, A. Le Moigne, M. Laban, K. Hackett, P. Weinerfelt, Aerodynamic considerations of blended wing body aircraft, Prog. Aerosp. Sci. 40 (6) (2004) 321–343, https://doi.org/10.1016/j.paerosci.2004.08.001.
[19] J. Hileman, Z. Spakovszky, M. Drela, M. Sargeant, Airframe design for 'silent aircraft', in: 45th AIAA Aerospace Sciences Meeting and Exhibit, Reno, Nevada, 2007.
[20] P. Li, B. Zhang, Y. Chen, C. Yuan, Y. Lin, Aerodynamic design methodology for blended wing body transport, Chin. J. Aeronaut. 25 (4) (2012) 508–516, https://doi.org/10.1016/S1000-9361(11)60414-7.
[21] P. Callewaert, S. Ghazi, R. Hageman, N. Kooiman, B. Lammens, E. Mobron, N.M. Nartey, R. van Osnabrugge, M. Yildirim, Multifuel Blended Wing Body, Delft University of Technology, Design Synthesis Exercise Report, Delft, The Netherlands, 2012.
[22] F. Yin, A.G. Rao, Off-design performance of an interstage turbine burner turbofan engine, J. Eng. Gas Turbines Power 139 (8) (2017) 082603, https://doi.org/10.1115/1.4035821, 8 pp.
[23] C. Huo, N.G. Diez, A.G. Rao, Numerical investigations on the conceptual design of a ducted contra-rotating Fan, in: ASME Turbo Expo 2014: Turbine Technical Conference and Exposition, 2014, V01AT01A028, 12 pp.
[24] A.G. Rao, A. Bhat, Hybrid combustion system for future aero engines, in: Proceedings of the 2nd National Propulsion Conference, IIT Bombay, Powai, Mumbai, 2015, pp. 1–9.
[25] F. Yin, A.G. Rao, Performance analysis of an aero engine with inter-stage turbine burner, Aeronaut. J. 121 (1245) (2017) 21, https://doi.org/10.1017/aer.2017.93.
[26] W.P. Visser, M.J. Broomhead, GSP, a generic object-oriented gas turbine simulation environment, in: ASME Turbo Expo 2010: Power for Land, Sea, and Air, Munich, Germany, 2000.
[27] GSP-Development-Team, GSP 11 User Manual – Version 11.1.0, National Aerospace Laboratory, The Netherlands, 2010.
[28] H.I.H. Saravanamuttoo, G.F.C. Rogers, H. Cohen, P.V. Straznicky, Gas Turbine Theory, 6th ed., Pearson Education Canada, Canada, 2008.
[29] P.P. Walsh, P. Flectcher, Gas Turbine Performance, 2nd ed., Blackwell Science, Oxford, UK, 2004.
[30] T. Lengyel-Kampmann, A. Bischoff, R. Meyer, E. Nicke, Design of an economical counter rotating fan: comparison of the calculated and measured steady and unsteady results, in: ASME Turbo Expo 2012: Turbine Technical Conference and Exposition, 2012, pp. 323–336.
[31] F.S. Tiemstra, Design of a Semi-Empirical Tool for the Evaluation of Turbine Cooling Requirements in a Preliminary Design Stage, Master thesis, Delft University of Technology, Delft, The Netherlands, 2014, http://resolver.tudelft.nl/uuid:225cfccd-2fc3-4a4d-a8a8-c24bd24bae44.
[32] F. Yin, F.S. Tiemstra, A.G. Rao, Development of a flexible turbine cooling prediction tool for preliminary design of gas turbines, J. Eng. Gas Turbines Power (2018), accepted in press.
[33] K.G. Fohmann, Design of a Cooling System for the Hybrid Engine: Design of a Heat Exchanger for Cooling Bleed Air with Liquefied Natural Gas, Master thesis, Delft University of technology, 2015, http://resolver.tudelft.nl/uuid:da4c2e09-fbbe-4690-9e52-86554550d3de.
[34] R.K. Shah, D.P. Sekulić, Fundamentals of Heat Exchanger Design, John Wiley & Sons, 2003.
[35] Piano-X, [cited 2015 4th August], Retrieved from: http://www.lissys.demon.co.uk/PianoX.html.
[36] V. Grewe, L. Bock, U. Burkhardt, K. Dahlmann, K.M. Gierens, L. Hüttenhofer, S. Unterstrasser, A. Rao, A. Bhat, F. Yin, T.G. Reichel, C.O. Paschereit, Y. Leshayahou, Assessing the climate impact of the AHEAD multi-fuel blended wing body, Meteorol. Z. 26 (6) (2017) 15, https://doi.org/10.1127/metz/2016/0758.